

Tetraquark Interpretation of the Charged Bottomonium-like states $Z_b^\pm(10610)$ and $Z_b^\pm(10650)$ and Implications

Ahmed Ali,^{*} Christian Hambrock,[†] and Wei Wang[‡]
Deutsches Elektronen-Synchrotron DESY, D-22607 Hamburg, Germany

We present a tetraquark interpretation of the charged bottomonium-like states $Z_b^\pm(10610)$ and $Z_b^\pm(10650)$, observed by the Belle collaboration in the $\pi^\pm\Upsilon(nS)$ ($n = 1, 2, 3$) and $\pi^\pm h_b(mP)$ ($m = 1, 2$) invariant mass spectra from the data taken near the peak of the $\Upsilon(5S)$. In this framework, the underlying processes involve the production and decays of a vector tetraquark $Y_b(10890)$, $e^+e^- \rightarrow Y_b(10890) \rightarrow [Z_b^\pm(10610)\pi^\mp, Z_b^\pm(10650)\pi^\mp]$ followed by the decays $[Z_b^\pm(10610), Z_b^\pm(10650)] \rightarrow \pi^\pm\Upsilon(nS), \pi^\pm h_b(mP)$. Combining the contributions from the meson loops and an effective Hamiltonian, we are able to reproduce the observed masses of the $Z_b^\pm(10610)$ and $Z_b^\pm(10650)$. The analysis presented here is in agreement with the Belle data and provides crucial tests of the tetraquark hypothesis. We also calculate the corresponding meson loop effects in the charm sector and find them dynamically suppressed. The charged charmonium-like states $Z_c^\pm(3752)$ and $Z_c^\pm(3882)$ can be searched for in the decays of the $J^{PC} = 1^{--}$ tetraquark state $Y(4260)$ via $Y(4260) \rightarrow Z_c^\pm(3752)\pi^\mp$ and $Y(4260) \rightarrow Z_c^\pm(3882)\pi^\mp$, with the subsequent decays $(Z_c^\pm(3752), Z_c^\pm(3882)) \rightarrow (J/\psi, h_c)\pi^\pm$.

PACS numbers: 14.40Pq, 13.66Bc, 14.40Rt

Recently Belle [1] (updating a previous publication [2]) reported the measurement of the $\pi^\pm\Upsilon(nS)$ ($n = 1, 2, 3$) and $\pi^\pm h_b(mP)$ ($m = 1, 2$) invariant mass spectra from the data taken near the peak of the $\Upsilon(5S)$ resonance in the processes $e^+e^- \rightarrow \Upsilon(nS)\pi^+\pi^-$ and $e^+e^- \rightarrow h_b(mP)\pi^+\pi^-$, in which two charged bottomonium-like states $Z_b^\pm(10610)$ and $Z_b^\pm(10650)$ are discovered. Hereafter, these states will be abbreviated to Z_b and Z'_b , respectively. The masses and decay widths averaged over the five different final states are in MeV [1]:

$$m_{Z_b^\pm} = 10607.2 \pm 2.0, \quad m_{Z'_b} = 10652.2 \pm 1.5, \\ \Gamma_{Z_b^\pm} = 18.4 \pm 2.4, \quad \Gamma_{Z'_b} = 11.5 \pm 2.2.$$

The angular distribution analysis indicates that the quantum numbers of both Z_b^\pm and Z'_b are $I^G(J^P) = 1^+(1^+)$. These states defy a standard bottomonium assignment, as in the valence approximation they consist of four quarks $bub\bar{b}\bar{d}$ (and charge conjugates).

Due to the proximity of the Z_b and Z'_b masses with the $B\bar{B}^*$ and $B^*\bar{B}$ thresholds [3], it has been proposed that the former could be realized as S -wave $B\bar{B}^*$ and $B^*\bar{B}$ molecular states, respectively [4–10]. In this scenario, the heavy quark spin structure of the Z_b and Z'_b is expected to mimic that of the corresponding meson pairs

$$|Z'_b\rangle = (0_{bb}^- \otimes 1_{q\bar{q}}^- - 1_{bb}^- \otimes 0_{q\bar{q}}^-)/\sqrt{2}, \\ |Z_b\rangle = (0_{bb}^- \otimes 1_{q\bar{q}}^- + 1_{bb}^- \otimes 0_{q\bar{q}}^-)/\sqrt{2}, \quad (1)$$

where 0^- and 1^- denotes the para and ortho- states with negative parity, respectively. One anticipates the mass splitting to follow $\Delta m_{Z_b} \equiv m_{Z'_b} - m_{Z_b} = m_{B^*} - m_B \simeq 46$

MeV, in neat agreement with the observed value $\Delta m_{Z_b} = (45 \pm 2.5)$ MeV [1]. Moreover, the structure in Eq. (1) predicts that Z_b and Z'_b should have the same decay width, which is approximately in agreement with the data.

Despite these striking patterns, the fact that both Z_b and Z'_b lie nominally above their respective thresholds by about 2 MeV reveals a tension with the molecular interpretation. If consolidated by more precise experiments, this feature may become a serious problem in this approach, as a one-pion exchange potential, which would produce such a bound state, does not support an S -wave $B\bar{B}^*$ resonance above threshold in an effective field theory [11]. Also, the measured total decay widths appear much too large compared to the naively expected ones for loosely bound states, and this suggests that both Z_b and Z'_b are compact hadrons. In addition, the measured cross sections in question are too big to be interpreted in terms of the decays $\Upsilon(5S) \rightarrow (\Upsilon(nS), h_b(mP))\pi^+\pi^-$.

In this paper, we pursue a different ansatz in which the observed processes arise from the production and decays of a vector tetraquark $Y_b(10890)$ [12–14], having a (Breit-Wigner) resonant mass of $[10888.4^{+2.7}_{-2.6}(\text{stat}) \pm 1.2(\text{syst})]$ MeV and a width of $[30.7^{+8.3}_{-7.0}(\text{stat}) \pm 3.1(\text{syst})]$ MeV [15, 16]. The mass and, in particular, the decay width of $Y_b(10890)$ differ from the Particle Data Group entries assigned to the $\Upsilon(5S)$ [3]. We propose that the states Z_b and Z'_b seen in the decays of $Y_b(10890)$ are themselves charged tetraquark candidates having the flavor configuration $[bu][\bar{b}\bar{d}]$ (and charge conjugates) (see Refs. [17, 18] for earlier suggestions along these lines). Their neutral isospin counterparts with $I_3 = 0$ have $J^{PC} = 1^{+-}$ and their masses were calculated in the effective Hamiltonian approach in [12]. Ignoring the small isospin-breaking effects [12, 19], Z_b and Z'_b have the same masses as those of their neutral counterparts. As shown below, these estimates yield a too large value for Δm_{Z_b} compared to the Belle measurement.

However, threshold effects and common decay chan-

^{*} ahmed.ali@desy.de

[†] christian.hambrock@desy.de

[‡] wei.wang@desy.de

nels may play an important role beyond what can be described by the constituent quark model and its transcribed form adopted in [19] to work out the spectroscopic aspects for the tetraquark states. In particular, two hadronic states having the same quantum numbers may mix due to dynamical effects, leading to differences in their masses and decay widths. Typically, the resulting mass shift is dominated by decays to the common states and reflects the partial widths to these states. A case in point here is the mass difference between the D^0 and \bar{D}^0 , which is dominated by such common decay channels, and is usually calculated by the meson loops, as dictated by the optical theorem [20]. Following essentially the same line of argument, we quantify this effect for the two charged-bottomonium-like states Z_b^\pm and $Z'_b{}^\pm$. We recalculate the masses of Z_b and Z'_b states by taking into account the meson loop contributions involving the Zweig-allowed two-body intermediate states $B\bar{B}^*$, $B^*\bar{B}$, $h_b(mP)\pi$, $\Upsilon(nS)\pi$ and $\eta_b\rho$. Theoretical estimates presented here account for the observed masses; in particular, the precisely measured mass difference Δm_{Z_b} is reproduced in terms of the partial decay widths of Z_b and Z'_b . This can be tested in future when the partial decay widths are measured precisely. In our approach, the mass eigenstates Z_b and Z'_b are rotated with respect to the tetraquark spin states \tilde{Z}_b and \tilde{Z}'_b , and we determine this mixing angle.

We also work out the corresponding meson loop effects for the charged charmonium-like states Z_c^\pm and $Z'_c{}^\pm$, with each one of them belonging to an isotriplet. The masses of the electrically neutral states have been calculated and are predicted to have typical values $m(Z_c) = 3752$ MeV and $m(Z'_c) = 3882$ MeV [19]. Ignoring the small isospin-breaking effects, these estimates apply for the charged counterparts Z_c^\pm and $Z'_c{}^\pm$ as well. We find that the meson-loop effects are in this case dynamically suppressed, as detailed below. However, we do expect that the production and decays of the Z_c^\pm and $Z'_c{}^\pm$ will essentially mimic the patterns seen for their bottomonium counterparts Z_b^\pm and $Z'_b{}^\pm$. In particular, Z_c^\pm and $Z'_c{}^\pm$, which are not measured so far, can be searched for in the decays of the neutral $J^{PC} = 1^{--}$ state $Y(4260)$, via the processes $Y(4260) \rightarrow Z_c^\pm(3752)\pi^\mp$ and $Y(4260) \rightarrow Z'_c{}^\pm(3882)\pi^\mp$, with the subsequent decays $(Z_c^\pm(3752), Z'_c{}^\pm(3882)) \rightarrow (J/\psi, h_c)\pi^\pm$.

We start with the classification of the \tilde{Z}_b and \tilde{Z}'_b tetraquark states in terms of the spin and orbital angular momentum of the constituent diquark and antidiquark. The concept of diquark was introduced by Gellmann in his epochal paper on quarks [21] and since then has been widely discussed in the literature (for reviews on diquarks, see Refs. [22, 23]). A diquark has positive parity and may be a scalar (spin-0, or “good” diquark) or an axial-vector (spin-1, or “bad” diquark) [24–26] and is assumed to be a color antitriplet $\bar{\mathbf{3}}_c$. The states \tilde{Z}_b and \tilde{Z}'_b arise from the production and decays of $Y_b(10890)$, identified with a linear combination of the two tetraquark states $Y_{[bq]} = [bq][\bar{b}\bar{q}]$ ($q = u, d$) having the spin and or-

bit momentum quantum numbers: $S_{[bq]} = 0$, $S_{[\bar{b}\bar{q}]} = 0$, $S_{[bq][\bar{b}\bar{q}]} = 0$, $L_{[bq][\bar{b}\bar{q}]} = 1$, with the total spin $J_{[bq][\bar{b}\bar{q}]} = 1$ [12]. We shall be using a non-relativistic notation to characterize the tetraquark states $|S_{[bq]}, S_{[\bar{b}\bar{q}]}; J_{[bq][\bar{b}\bar{q}]}\rangle$, in which a matrix representation of the interpolating operators is used in terms of the 2×2 Pauli matrices σ_i ($i = 1, 2, 3$): $0_{[Q\bar{Q}]} \equiv Q^T \sigma_2 Q / \sqrt{2}$, $1_{[Q\bar{Q}]} \equiv Q^T \sigma_2 \sigma^i Q / \sqrt{2}$ and $0_{Q\bar{Q}} \equiv \bar{Q} Q / \sqrt{2}$, $1_{Q\bar{Q}} \equiv \bar{Q} \sigma^i Q / \sqrt{2}$, Q being any quark. The two tetraquark spin states \tilde{Z}_b and \tilde{Z}'_b are represented as

$$\begin{aligned} |\tilde{Z}_b\rangle &= (0_{[bq]} \otimes 1_{[\bar{b}\bar{q}]} - 1_{[bq]} \otimes 0_{[\bar{b}\bar{q}]}) / \sqrt{2}, \\ |\tilde{Z}'_b\rangle &= 1_{[bq]} \otimes 1_{[\bar{b}\bar{q}]} . \end{aligned} \quad (2)$$

Performing a Fierz transformation, the flavor and spin content in the $b\bar{b} \otimes q\bar{q}$ and $b\bar{q} \otimes q\bar{b}$ product space can be made explicit:

$$\begin{aligned} |\tilde{Z}_b\rangle &= (-1_{b\bar{b}}^- \otimes 0_{q\bar{q}}^- + 0_{b\bar{b}}^- \otimes 1_{q\bar{q}}^-) / \sqrt{2} = 1_{b\bar{q}}^- \otimes 1_{q\bar{b}}^-, \\ |\tilde{Z}'_b\rangle &= (1_{b\bar{b}}^- \otimes 0_{q\bar{q}}^- + 0_{b\bar{b}}^- \otimes 1_{q\bar{q}}^-) / \sqrt{2} \\ &= (1_{b\bar{q}}^- \otimes 0_{q\bar{b}}^- + 0_{b\bar{q}}^- \otimes 1_{q\bar{b}}^-) / \sqrt{2}. \end{aligned} \quad (3)$$

Eq. (3) shows that the \tilde{Z}_b and \tilde{Z}'_b have similar coupling strengths with different final states. The labels $0_{b\bar{q}}$ and $1_{b\bar{q}}$ in Eq. (3) can be viewed as \bar{B} and \bar{B}^* , respectively. It follows that \tilde{Z}_b couples to $B^*\bar{B}^*$ state while \tilde{Z}'_b couples to $\bar{B}\bar{B}^*$. We stress that this identification is in contrast with the molecular interpretation, in which the transition $\tilde{Z}'_b \rightarrow \bar{B}\bar{B}^* + h.c.$ is forbidden by the spin symmetry since \tilde{Z}'_b is assumed to be essentially a $B^*\bar{B}^*$ molecule [4]. This difference can be tested in the future and is of great importance in order to distinguish between the tetraquark and the hadronic molecule interpretations.

In the effective Hamiltonian approach, the 2×2 mass matrix for the S -wave 1^+ tetraquarks \hat{M} is given by [19]

$$\hat{M} = \left(2m_{[bq]} + \frac{3}{2}\Delta - \frac{\kappa_{q\bar{q}} + \kappa_{b\bar{b}}}{2} \right) \mathbb{I} + \begin{pmatrix} -a & b \\ b & a \end{pmatrix}, \quad (4)$$

where \mathbb{I} is a 2×2 unit matrix, $a = \Delta/2 + (\kappa_{bq})_{\bar{3}} - \kappa_{b\bar{q}}$ and $b = \kappa_{q\bar{q}} - \kappa_{b\bar{b}}$. In the above $(\kappa_{bq})_{\bar{3}}$ accounts for the spin-spin interaction between the quarks inside the diquark and antidiquark, $\kappa_{q\bar{q}}$ and $\kappa_{b\bar{b}}$ are the couplings accounting for the interaction between the quarks in the diquark to the antiquarks in the antidiquark, and Δ is the mass difference between the spin-1 and spin-0 diquarks. Using the default values of the parameters [12, 13] (in units of MeV)

$$\kappa_{q\bar{q}} = 79.5, \quad \kappa_{b\bar{b}} = 9, \quad \kappa_{b\bar{q}} = 5.75, \quad (\kappa_{bq})_{\bar{3}} = 6, \quad (5)$$

yields the diquark mass $m_{[bq]} \simeq 5200$ MeV (from the $Y_b(10890)$ mass). The value of Δ is uncertain, with $\Delta \simeq 200$ MeV for the light quarks [26]. Reducing its value drastically for the c and b quarks will reduce the level spacing of the corresponding tetraquark states for which the experimental evidence is rather sparse. Due to the lack of data, we adopt an admittedly somewhat arbitrary

range $\Delta = (120 \pm 30)$ MeV for our numerical calculations. These parameters yield the following values for the two charged tetraquark masses and the mass difference

$$\begin{aligned} m_{Z_b} &= (10443_{-36}^{+35})\text{MeV}, \quad m_{Z'_b} = (10628_{-54}^{+53})\text{MeV}, \\ \Delta m_{Z_b} &= 2\sqrt{a^2 + b^2} = (185_{-18}^{+21})\text{MeV}. \end{aligned} \quad (6)$$

We note that the prediction for Δm_{Z_b} given above is much larger than the experimental data, and there is no easy-fix for this mismatch at hand in terms of the parameters in the effective Hamiltonian. Since this Hamiltonian [19] adequately describes the mass spectrum of the exotic states discovered in the charm sector, we continue to use this as our starting point and argue that additional dynamical contributions to the mass matrix arise from the meson loops.

With this premise, the renormalized masses can be obtained by computing the two-point functions. At the one-loop level, the self-energy corrections to the unperturbed propagator $\Sigma(p^2)g_{\mu\nu}$, depicted in Fig. 1, are written as

$$\frac{-i(g^{\mu\alpha} - p^\mu p^\alpha/p^2)}{p^2 - \hat{M}^2} i\Sigma(p^2)g_{\alpha\beta} \frac{-i(g^{\beta\nu} - p^\beta p^\nu/p^2)}{p^2 - \hat{M}^2}. \quad (7)$$

Taking the $h_b\pi$ state as an example, we find

$$\Sigma(s) = \frac{g_{\tilde{Z}_b^{(\prime)} h_b \pi} g_{\tilde{Z}'_b^{(\prime)} h_b \pi}}{(4\pi)^2} \int_0^1 dx s \Lambda \left[1 - \log\left(\frac{\Lambda}{\mu^2}\right) \right], \quad (8)$$

where $\Lambda = x^2 s - xs + xm_\pi^2 + (1-x)m_{h_b}^2 - i\epsilon$, and the coupling constants appearing above are defined through the hadronic interaction

$$\mathcal{L} = \epsilon_{\mu\nu\alpha\beta} g_{\tilde{Z}_b^{(\prime)} h_b \pi} \partial^\mu \tilde{Z}_b^{(\prime)\nu} \partial^\alpha h_b^\beta \pi + h.c.. \quad (9)$$

In deriving $\Sigma(s)$, the $\overline{\text{MS}}$ scheme in the unitarity gauge has been used to remove the UV divergence with the scale $\mu \sim m_{Z_b^{(\prime)}}$. We recall that the real parts of $\Sigma(s)$ contribute to the mass matrix, while the imaginary parts of $\Sigma(s)$ are related to the decay widths of \tilde{Z}_b and \tilde{Z}'_b . In particular, the transitions $\tilde{Z}_b \rightarrow (\Upsilon(nS)\pi, h_b(mP)\pi, \eta_b(nS)\rho) \rightarrow \tilde{Z}'_b$ contribute to the off-diagonal terms in the 2×2 mass matrix and provide significant effects on the mixing of the two tetraquark-spin eigenstates.

The meson loop corrections due to the different hadronic channels can be viewed as renormalizing the ‘‘bare’’ mass for the states predicted in the constituent tetraquark model. We are interested in the relative mass shifts which are reflected by the genuine part of the loop contributions $\text{Re}\Sigma_{gen}(s)$. These can be obtained by a subtraction procedure at a suitable mass scale s_0 [27]:

$$\text{Re}\Sigma_{gen}(s) = \text{Re}\Sigma(s) - \text{Re}\Sigma(s_0). \quad (10)$$

Setting the scale s_0 needs a prescription. It is reasonable to choose s_0 as the mass squared of the lowest lying bound state for a given quark flavor, which we take as the $J^{PC} = 0^{++}$ scalar tetraquark state. A different choice,

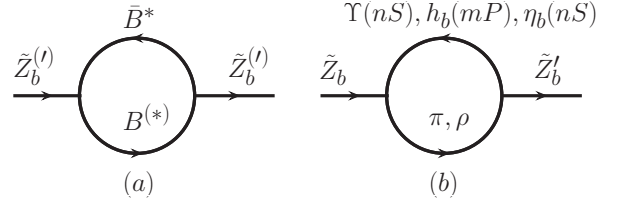


FIG. 1. Two-body meson-loop corrections to the function $\Sigma(s)$ defined in Eq. (8). The intermediate states $B^{(*)}\bar{B}^*$ contribute only to the diagonal terms in the mass matrix while $\Upsilon(nS)\pi$, $h_b(mP)\pi$ and $\eta_b(nS)\rho$ contribute to both the diagonal and non-diagonal terms.

namely $s_0 = 4m_{[bq]}^2$, will slightly modify our results and the effects caused by the ambiguity in s_0 will be incorporated in estimating the systematic uncertainties in our approach.

Including the loop corrections, we now have the following structure for the 2×2 mass matrix

$$M = \hat{M} + \sum_i c_i \begin{pmatrix} \Gamma_i^{\tilde{Z}_b} & -\sqrt{\Gamma_i^{\tilde{Z}_b} \Gamma_i^{\tilde{Z}'_b}} \\ -\sqrt{\Gamma_i^{\tilde{Z}_b} \Gamma_i^{\tilde{Z}'_b}} & \Gamma_i^{\tilde{Z}'_b} \end{pmatrix}, \quad (11)$$

where i runs over the two-body channels shown in Fig. 1; the coefficients $c_i(s, s_0)$ are defined as

$$c_i(s, s_0) \equiv -\frac{\text{Re}\Sigma_{gen}(s)}{2 \text{Im}\Sigma(s)}, \quad (12)$$

in which s is taken as the physical mass squared from the data and $\text{Re}\Sigma_{gen}(s)$ is determined as in Eq. (10). The sign in the $\Upsilon(nS)\pi$ contributions to the off-diagonal terms is reversed due to the spin symmetry as shown in Eq. (3). In the case of open bottom mesons, the $B\bar{B}^*$ loop impacts on M_{22} while $B^*\bar{B}$ modifies M_{11} . Note, that via the optical theorem the imaginary parts are directly related to the decay widths, and our parametrization in Eq. (11) makes this manifest.

Choosing the subtraction point as $s_0 = [(10.385 \pm 0.05)\text{GeV}]^2$, which corresponds to the mass of the lowest (0^{++}) tetraquark state with a hidden $b\bar{b}$ quark content, we estimate the following values for the coefficients c_i (ignoring errors on the smaller c_i s):

$$\begin{array}{|c|c|c|c|} \hline |c_{h_b(2P)\pi}| & |c_{\eta_b\rho}| & |c_{h_b(1P)\pi}| & |c_{B\bar{B}^*}| \\ \hline |45_{-10}^{+11}| & |-1.1| & |3 \pm 1| & |-1.1| \\ \hline \end{array}$$

For the analysis of $\Upsilon(nS)\pi$ contribution, the Lagrangian $\mathcal{L} = g_{V Z_b^{(\prime)} \pi} V^\mu Z_{b\mu}^{(\prime)} \pi$ with $V = Y_b, \Upsilon(nS)$ gives

$$\begin{aligned} \Sigma(s) &= -\frac{g_{\tilde{Z}_b^{(\prime)} \Upsilon(nS)\pi} g_{\tilde{Z}'_b^{(\prime)} \Upsilon(nS)\pi}}{(4\pi)^2} \int_0^1 dx \left[-\log\left(\frac{\Lambda}{\mu^2}\right) \right. \\ &\quad \left. + \frac{\Lambda}{2m_{\Upsilon(nS)}^2} \log\left(\frac{\Lambda}{\mu^2}\right) - \frac{\Lambda}{2m_{\Upsilon(nS)}^2} \right], \end{aligned} \quad (13)$$

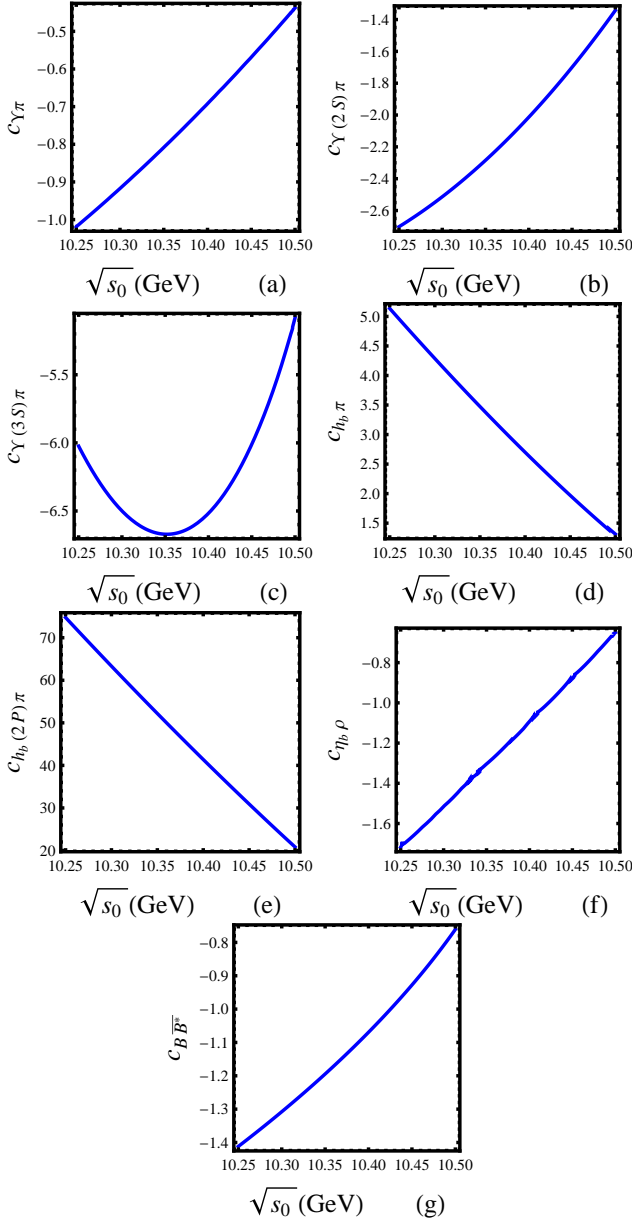


FIG. 2. Dependence of the coefficients c_i on the subtraction scale s_0 calculated with the Lagrangian in Eq. (15). The frames (a) to (g) correspond to the intermediate states $i = \Upsilon(1S)\pi, \Upsilon(2S)\pi, \Upsilon(3S)\pi, h_b(1P)\pi, h_b(2P)\pi, \eta_b\rho, B\bar{B}^*$, respectively.

with $\Lambda = x^2s - xs + xm_\pi^2 + (1-x)m_{\Upsilon(nS)}^2 - i\epsilon$ and the relevant coefficients are predicted as

$$\begin{aligned} c_{\Upsilon(1S)\pi} &= -0.01, & c_{\Upsilon(2S)\pi} &= -0.1, \\ c_{\Upsilon(3S)\pi} &= -1.3. \end{aligned} \quad (14)$$

The expression for contributions from the $Z_b^{(\prime)} \rightarrow \eta_b\rho$ channel is similarly obtained by replacing the vector $\Upsilon(nS)$ by ρ and the pseudoscalar π by η_b .

Instead of the Lagrangian specified above, using the

Lagrangian with the derivative of the pion field which is inspired by the chiral symmetry

$$\mathcal{L} = g_V Z_b^{(\prime)\pi} V^\mu i \overleftrightarrow{\partial}_\nu Z_{b\mu}^{(\prime)} i \partial^\nu \pi, \quad (15)$$

we have

$$\begin{aligned} \Sigma(s) &= -\frac{g_{Z_b^{(\prime)}\Upsilon(nS)\pi} g_{Z_b^{(\prime)}\Upsilon(nS)\pi}^*}{(4\pi)^2} \int_0^1 dx \\ &\times \left\{ \frac{\Lambda^3}{4m_{\Upsilon(nS)}^2} \left[4 \log\left(\frac{\Lambda}{\mu^2}\right) - 5 \right] \right. \\ &- \frac{\Lambda^2}{4m_{\Upsilon(nS)}^2} \left[3(4m_{\Upsilon(nS)}^2 + s(2-3x^2)) \log\left(\frac{\Lambda}{\mu^2}\right) - \right. \\ &- 8m_{\Upsilon(nS)}^2 + 12sx^2 - 7s \left. \right] \\ &+ \frac{\Lambda s}{2m_{\Upsilon(nS)}^2} \left[[(8x^2-4)m_{\Upsilon(nS)}^2 - (x^2-1)^2 s] \right. \\ &+ \left. \left. [(8-12x^2)m_{\Upsilon(nS)}^2 + s(1-x^2)^2] \log\left(\frac{\Lambda}{\mu^2}\right) \right] \right. \\ &\left. - s^2(x^2-1)^2 \log\left(\frac{\Lambda}{\mu^2}\right) \right\}. \end{aligned} \quad (16)$$

This expression yields larger values for the coefficients $c_{\Upsilon(nS)\pi}$:

$$\begin{aligned} c_{\Upsilon(1S)\pi} &= -0.7, & c_{\Upsilon(2S)\pi} &= -2.1, \\ c_{\Upsilon(3S)\pi} &= -6.5. \end{aligned} \quad (17)$$

It should be noted that these numbers are much larger than the ones in Eq. (14), due to the fact that the pion momentum coming from the derivative in Eq. (15) is small in the $Z_b^{(\prime)}$ rest frame and thus suppresses the partial decay width and hence the denominator in the definition of c_i as in Eq. (12).

The dependence of these coefficients on the subtraction scale is shown in Fig. 2, where the Lagrangian in Eq. (15) has been used. The striking result is that the coefficient $c_{h_b(2P)\pi}$ dominates by far all the others. The main reason for the dominance of the coefficient $c_{h_b(2P)\pi}$ is that the limited phase space and the p-wave decay character of $Z_b^{(\prime)} \rightarrow h_b(2P)\pi$ result in a comparably small value for the imaginary part of $\Sigma(s)$ compared to its real part. In Ref. [28], Belle collaboration has reported the measurements of the cross sections for $e^+e^- \rightarrow \Upsilon(nS)\pi^+\pi^-$ and $e^+e^- \rightarrow h_b(mP)\pi^+\pi^-$ near the peak of the $\Upsilon(5S)$ resonance. Using the final state $\Upsilon(2S)\pi^+\pi^-$ as normalization, they found that the ratios of the various cross sections are typically all of order 1. Thus, the partial widths for the different final states listed are comparable, which suggests a value of $O(1)$ MeV for each of them [1]. Thus, the domination of the $h_b(2P)\pi$ channel in the meson-loop corrections to the 1^{+-} mass matrix is a consequence of this channel having the largest coefficient and the anticipated sizable partial decay width of $Z_b^{(\prime)} \rightarrow h_b(2P)\pi$. This is worked out quantitatively later.

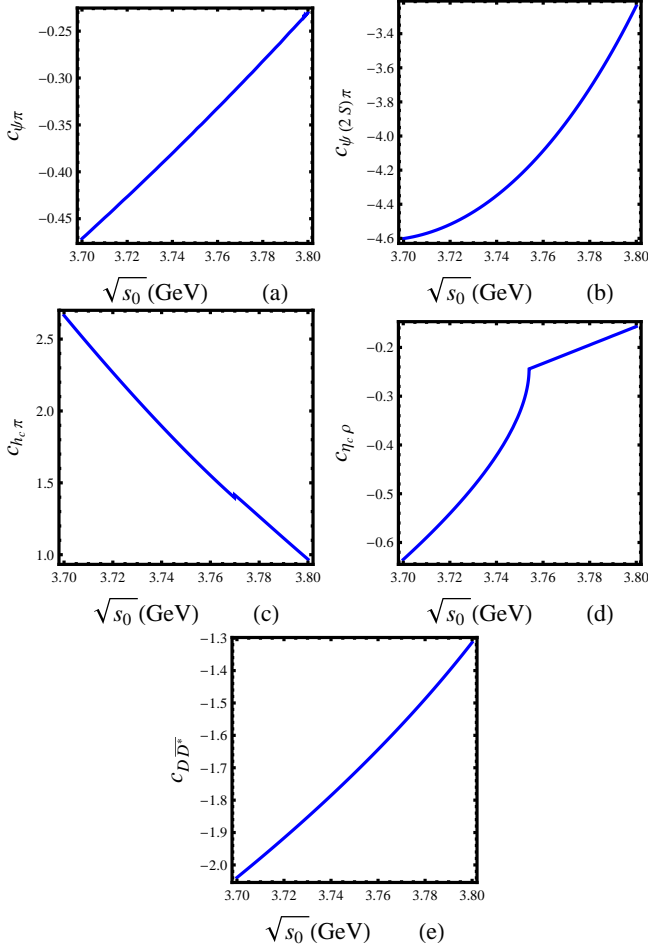


FIG. 3. Dependence of the coefficients c_i for hadronic decay channels of the charmonium-like $Z_c^{(\prime)}$ states on the subtraction scale s_0 calculated with the Lagrangian in Eq. (15). The panels (a) to (e) correspond to the intermediate states $i = J/\psi\pi, \psi(2S)\pi, h_c\pi, \eta_c\rho, D\bar{D}^*$, respectively.

For comparison, we have performed the same calculation for the hidden-charm tetraquark states whose masses are calculated in the constituent diquark model by Maiani et al. [19], predicting the masses of the two 1^{+-} $c\bar{c}$ hidden tetraquark states as

$$m_{Z_c} = 3.752 \text{ GeV}, \quad m_{Z_c'} = 3.882 \text{ GeV}. \quad (18)$$

This yields a mass difference $\Delta m_{Z_c} = 130$ MeV. Ignoring the isospin symmetry breaking effects, typically a few MeV, the above estimates hold also for the charged counterparts. Since the above masses are very close to the estimate of the mass of the lightest scalar $J^{PC} = 0^{++}$ tetraquark state, $m_{S_c} = 3.723$ GeV [19], the genuine meson-loop contributions, after subtraction, are expected to be small. We show the corresponding coefficients for various hadronic channels in Fig. 3, where in order to determine the imaginary part the mass for the higher 1^{+-} state has been used as the physical mass. A striking difference between the coefficients shown in Figs. 2 and 3

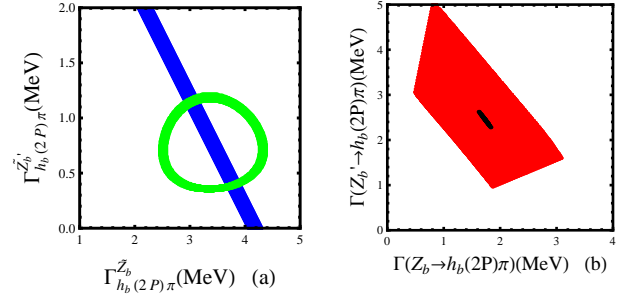


FIG. 4. Constrained partial decay widths from the Z_b and Z_b' masses measured by Belle. The left-hand panel shows the constraint on the partial decay widths of the tetraquark eigenstates \tilde{Z}_b and \tilde{Z}_b' . The circular (green) contour is obtained by the mass difference $\Delta m_{Z_b} = 45 \pm 2.5$ MeV, while the slanted vertical (blue) band results from the averaged mass $(m_{Z_b} + m_{Z_b'})/2 = 10629.7 \pm 2.5$ MeV for the default values $\Delta = 120$ MeV and $c_{h_b(2P)\pi} = 45$. In the right-hand panel, the corresponding constraints on Z_b and Z_b' partial decay widths are depicted. The solid (black) region results from default values, while the extended (red) region is obtained by varying these two parameters, as stated in the text.

is the absence of the coefficient $c_{h_c(2P)\pi}$ in Fig. 3, as the decays $Z_c^{(\prime)} \rightarrow h_c(2P)\pi$ are not allowed kinematically. Assuming that the partial decay widths in the various channels $J/\psi\pi, \psi(2S)\pi, h_c(1P)\pi, \eta_c\rho$ etc. are of order 1 MeV, as in the decays of the $Z_b^{(\prime)}$, we anticipate that the corrections due to the meson loops in the $Z_c - Z_c'$ mixing are also typically of the same order, namely order 1 MeV, hence not significant. Thus, unlike the masses of the $Z_b - Z_b'$ complex, the masses for the hidden-charm tetraquarks calculated in Ref. [19] are not expected to be significantly modified by meson-loop effects.

As already remarked, the 1^{+-} relatives of the Z_b and Z_b' states in the charm sector, Z_c and Z_c' , in our model are expected to be produced in the decays of a 1^{--} hidden-charm tetraquark. The state $Y(4260)$ fits the bill. The enhancement of the cross sections for $e^+e^- \rightarrow J/\psi\pi^+\pi^-$ and $e^+e^- \rightarrow h_c\pi^+\pi^-$ seen by the CLEO collaboration at the center-of-mass energy around 4.26 GeV [29] is very likely a signature of their existence. In order to confirm or negate this scenario, we suggest our experimental colleagues to scan over this mass region more precisely.

Returning to the discussion of the mass difference of the 1^+ tetraquarks in the hidden $b\bar{b}$ sector, we note that it is approximately given as $\Delta m_{Z_b} = 2\sqrt{a'^2 + b'^2}$, where $a' = a - c_i(\Gamma_i^{\tilde{Z}_b} - \Gamma_i^{\tilde{Z}_b'})/2$, $b' = b - c_i\sqrt{\Gamma_i^{\tilde{Z}_b}\Gamma_i^{\tilde{Z}_b'}}$ and i denotes $h_b(2P)\pi$, as we keep only the dominant contribution. The corresponding mass eigenstates are

$$\begin{aligned} |Z_b\rangle &= \cos\theta_{Z_b}|\tilde{Z}_b\rangle - \sin\theta_{Z_b}|\tilde{Z}_b'\rangle, \\ |Z_b'\rangle &= \sin\theta_{Z_b}|\tilde{Z}_b\rangle + \cos\theta_{Z_b}|\tilde{Z}_b'\rangle, \end{aligned} \quad (19)$$

with $\theta_{Z_b} = \tan^{-1}[b'/(a' + \Delta m_{Z_b}/2)]$.

In Fig. 4, we show the constrained partial decay widths

from the masses observed by Belle. The left panel shows the constraints on the widths of the tetraquark mass eigenstates $\tilde{Z}_b^{(\prime)}$ for the default values of Δ and $c_{h_b(2P)\pi}$. In the spin-symmetry limit, $\Gamma_i^{\tilde{Z}_b}$ and $\Gamma_i^{\tilde{Z}'_b}$ are equal. As seen in this panel, the resulting contours intersect at two regions, the lower one of which implies large symmetry breaking effects and hence is not entertained any further. The upper region in which the two couplings differ by approximately 40% is further analyzed. In the right-hand panel, the corresponding constraints on the Z_b and Z'_b partial decay widths are depicted. The black region denotes the default values of Δ and c_i given above, while the extended (red) region is obtained by the variations of these two parameters in the ranges $\Delta = (120 \pm 30)\text{MeV}$ and $c_{h_b(2P)\pi} = 45^{+11}_{-10}$. Based on this, we estimate

$$\begin{aligned}\theta_{Z_b} &= (-19^{+13}_{-17})^\circ, \\ \Gamma(Z_b \rightarrow h_b(2P)\pi) &= (1.7^{+1.3}_{-1.2})\text{MeV}, \\ \Gamma(Z'_b \rightarrow h_b(2P)\pi) &= (2.5^{+2.5}_{-1.5})\text{MeV}.\end{aligned}\quad (20)$$

We note that the mixing angle is small, implying that the mass eigenstates are close to their respective tetraquark spin states. From the partial widths given above, we extract the relative strength of the coupling constants

$$r_{h_b(2P)\pi} \equiv |g_{Z'_b h_b(2P)\pi}/g_{Z_b h_b(2P)\pi}| = 1.2^{+1.1}_{-0.5}. \quad (21)$$

In the Belle data [1], the ratio $r_{h_b(2P)\pi}$ is not measured directly; what is reported is the ratio $a_i e^{i\phi_i} \equiv g_{Y_b Z'_b \pi} \times g_{Z'_b i} / (g_{Y_b Z_b \pi} \times g_{Z_b i})$, which are products of the production and the corresponding decay amplitudes of the Z_b and Z'_b in the given final states. The updated value in [1] is $a_{h_b(2P)\pi} = 1.6^{+0.6+0.4}_{-0.4-0.6}$. An analysis to estimate the relative amplitudes in all five final states reported in Table I in [1] is in progress in the tetraquark context. We anticipate that the couplings in the production amplitudes involving Z_b and Z'_b are similar, i.e., $|g_{Y_b Z'_b \pi}| \simeq |g_{Y_b Z_b \pi}|$ and hence $r_{h_b(2P)\pi} = a_{h_b(2P)\pi}$, in agreement with the Belle data.

Using the Lagrangian given in Eqs. (9) and (15), we have the following amplitudes for the decays $Y_b \rightarrow \Upsilon(nS)\pi^+\pi^-$ and $Y_b \rightarrow h_b(mP)\pi^+\pi^-$

$$\begin{aligned}i\mathcal{M}(Y_b \rightarrow \Upsilon(nS)\pi^+\pi^-) &= A_{nZ_b} + ig_{Y_b Z_b \pi} g_{Z_b} \Upsilon(nS)\pi \\ \epsilon_{Y_b} \cdot \epsilon_{\Upsilon(nS)}^* &\{(\text{BW}_{Z_b}^{\Upsilon(nS)\pi^+} + a_{\Upsilon(nS)\pi} e^{i\phi_{\Upsilon(nS)\pi}} \text{BW}_{Z'_b}^{\Upsilon(nS)\pi^+}) \\ &(m_{Y_b}^2 - p_{\Upsilon(nS)\pi^+}^2)(p_{\Upsilon(nS)\pi^+}^2 - m_{\Upsilon(nS)}^2) + (\pi^+ \rightarrow \pi^-)\}, \\ i\mathcal{M}(Y_b \rightarrow h_b(mP)\pi^+\pi^-) &= A'_{nZ_b} - ig_{Y_b Z_b \pi} g_{Z_b h_b \pi} \epsilon_{\mu\nu\alpha\beta} \\ \epsilon_{Y_b}^\nu p_{h_b(mP)}^\alpha \epsilon_{h_b(mP)}^{*\beta} &\{p_{\pi^+}^\mu (m_{Y_b}^2 - p_{h_b(mP)\pi^+}^2) [\text{BW}_{Z_b}^{h_b(mP)\pi^+} \\ &+ a_{h_b(mP)\pi} e^{i\phi_{h_b(mP)\pi}} \text{BW}_{Z'_b}^{h_b(mP)\pi^+}] + (\pi^+ \rightarrow \pi^-)\},\end{aligned}\quad (22)$$

with $\text{BW}_{Z_b}^{i(\prime)}$ $= [p_i^2 - m_{Z_b}^{2(\prime)} + im_{Z_b}^{(\prime)}\Gamma_{Z_b}^{(\prime)}]^{-1}$. Belle measurements show that the a_i s are roughly 1 within errors, while the phases ϕ_i are close to either 0 or 180°, though the errors are rather large. It is worth pointing out that the momentum dependence arising from the interaction

Lagrangian given in Eq. (15) are not taken into account in the parametrization adopted by Belle. Although the relative strength of the amplitudes, namely $a_i e^{i\phi_i}$, is not affected, the $\pi^\pm \Upsilon(nS)$ and $\pi^\pm h_b(mP)$ spectrum distributions will be modified. A_{nZ_b} and A'_{nZ_b} refer to the non- $Z_b^{(\prime)}$ amplitudes in the indicated final states.

The structure of A_{nZ_b} was worked out in the tetraquark picture in great detail in Refs. [13, 14]. As opposed to the amplitudes involved in typical dipionic heavy Quarkonia transitions, such as $\Upsilon(4S) \rightarrow \Upsilon(1S)\pi^+\pi^-$, which are modeled after the Zweig-suppressed QCD multipole expansion [30], the amplitudes for the decays $Y_b(10890) \rightarrow \Upsilon(nS)\pi^+\pi^-$ are not Zweig-forbidden, and hence they are significant. In addition, they lead to a resonant structure in the $\pi\pi$ invariant mass spectrum. This is most marked in the $\Upsilon(1S)\pi^+\pi^-$ mode in the form of the resonances $f_0(980)$ and $f_2(1270)$. The measured dipionic invariant mass spectra by Belle in these final states is in conformity with the predictions [13, 14]. On the other hand, the amplitudes A'_{nZ_b} in the decays $Y_b(10890) \rightarrow h_b(mP)\pi^+\pi^-$ are expected to be neither resonant nor numerically significant. Only the transition $Y_b(10890) \rightarrow h_b(1P)f_0(980)$ is marginally allowed, heavily suppressed by the phase space and the P -wave decay character. The state $f_0(600)$ (or $\sigma(600)$) contributes, in principle. However, as this is a very broad resonance, the higher mass part is again suppressed by the phase space and hence the contribution of the $f_0(600)$ in the decay $Y_b(10890) \rightarrow h_b(1P)f_0(600)$ is both small and difficult to discern. This feature is also in accord with the Belle data [1]. Finally, we note that the absence of any anomalous production of the states $(\Upsilon(nS)\pi^+\pi^-, h_b(mP)\pi^+\pi^-)$ in the decays of the bottomonium state $\Upsilon(11020)$ [16] is anticipated in the tetraquark picture, as opposed to the hadronic molecular interpretation of the Z_b and Z'_b for which the decays $\Upsilon(11020) \rightarrow Z_b^{(\prime)\pm}\pi^\mp \rightarrow \Upsilon(nS)\pi^+\pi^-, h_b(mP)\pi^+\pi^-$ are expected to be enhanced by the larger phase space compared to the corresponding decays from the $\Upsilon(5S)$.

In summary, we have presented a tetraquark interpretation of the two observed states $Z_b^\pm(10610)$ and $Z_b^\pm(10650)$. Combining the effective diquark-antidiquark Hamiltonian with the meson-loop induced effects, we are able to account for the observed masses in terms of the decay widths for the dominant channel $Z_b^{(\prime)\pm} \rightarrow h_b(2P)\pi^\pm$, obtaining a ratio for the relative decay amplitudes in the decays $Z_b^{(\prime)\pm} \rightarrow h_b(mP)\pi^\pm$ which agrees with the Belle data. Together with the resonant $\pi\pi$ structure in the decay modes $Y_b(10890) \rightarrow \Upsilon(nS)\pi^+\pi^-$, first worked out in [13, 14], this Letter provides additional support to the tetraquark hypothesis involving the states $Y_b(10890)$, $Z_b^\pm(10610)$ and $Z_b^\pm(10650)$. Precise spectroscopic measurements foreseen at the Super-B factories and at the LHC will provide definitive answers to several issues raised here and will help resolve the current and long-standing puzzles in the exotic bottomonium sector.

We acknowledge helpful discussions with Feng-kun

Guo and Satoshi Mishima. W. W. is supported by the Alexander-von-Humboldt Stiftung.

-
- [1] I. Adachi *et al.* [Belle Collaboration], arXiv:1110.2251.
 [2] I. Adachi *et al.* [Belle Collaboration], arXiv:1105.4583.
 [3] K. Nakamura *et al.* [Particle Data Group], J. Phys. G **37**, 075021 (2010).
 [4] A. E. Bondar, A. Garmash, A. I. Milstein, R. Mizuk and M. B. Voloshin, Phys. Rev. D **84**, 054010 (2011) [arXiv:1105.4473 [hep-ph]].
 [5] M. B. Voloshin, Phys. Rev. **D84**, 031502 (2011).
 [6] J. R. Zhang, M. Zhong, M. -Q. Huang, Phys. Lett. **B704**, 312-315 (2011).
 [7] Y. Yang *et al.*, arXiv:1105.5935.
 [8] Z. -F. Sun *et al.*, Phys. Rev. **D84**, 054002 (2011).
 [9] M. Cleven *et al.*, arXiv:1107.0254.
 [10] T. Mehen and J. W. Powell, arXiv:1109.3479 [hep-ph].
 [11] J. Nieves, M. P. Valderrama, arXiv:1106.0600.
 [12] A. Ali *et al.*, Phys. Lett. **B684**, 28-39 (2010).
 [13] A. Ali, C. Hambroek, M. J. Aslam, Phys. Rev. Lett. **104**, 162001 (2010).
 [14] A. Ali, C. Hambroek and S. Mishima, Phys. Rev. Lett. **106**, 092002 (2011).
 [15] K. F. Chen *et al.* [Belle Collaboration], Phys. Rev. Lett. **100**, 112001 (2008).
 [16] K. -F. Chen *et al.* [Belle Collaboration], Phys. Rev. **D82**, 091106 (R) (2010).
 [17] T. Guo *et al.*, arXiv:1106.2284.
 [18] C. -Y. Cui, Y. -L. Liu, M. -Q. Huang, arXiv:1107.1343.
 [19] L. Maiani *et al.*, Phys. Rev. **D71**, 014028 (2005).
 [20] J. F. Donoghue, E. Golowich, B. R. Holstein and J. Trampetic, Phys. Rev. D **33**, 179 (1986).
 [21] M. Gell-Mann, Phys. Lett. **8**, 214 (1964).
 [22] M. Anselmino, E. Predazzi, S. Ekelin, S. Fredriksson and D. B. Lichtenberg, Rev. Mod. Phys. **65**, 1199 (1993).
 [23] R. L. Jaffe, Phys. Rept. **409**, 1 (2005) [hep-ph/0409065].
 [24] R. L. Jaffe, Phys. Rev. D **15**, 281 (1977).
 [25] R. L. Jaffe and F. E. Low, Phys. Rev. D **19**, 2105 (1979).
 [26] R. L. Jaffe and F. Wilczek, Phys. Rev. Lett. **91**, 232003 (2003)
 [27] See, for example, M. R. Pennington and D. J. Wilson, Phys. Rev. D **76**, 077502 (2007).
 [28] I. Adachi *et al.* [Belle Collaboration], arXiv:1103.3419 [hep-ex].
 [29] T. K. Pedlar *et al.* [CLEO Collaboration], Phys. Rev. Lett. **107**, 041803 (2011) [arXiv:1104.2025 [hep-ex]].
 [30] For a recent review, see N. Brambilla *et al.*, Eur. Phys. J. **C71**, 1534 (2011).